

Sign of the hyperfine parameters of anomalous muonium in diamond

W. Odermatt, Hp. Baumeler, H. Keller, W. Kündig, B. D. Patterson, and J. W. Schneider
Physik-Institut, Universität Zürich, 8001 Zürich, Switzerland

J. P. F. Sellschop, M. C. Stemmet, and S. Connell
Nuclear Physics Research Unit, University of the Witwatersrand, Johannesburg 2001, South Africa

D. P. Spencer*
Physics Department, Rice University, Houston, Texas 77251
 (Received 24 August 1987; revised manuscript received 21 March 1988)

Observations with the muon-spin-rotation (μ SR) technique of the thermally activated transition from the isotropic muonium state Mu to the anisotropic muonium state Mu^* in diamond are used to determine the sign of the Mu^* hyperfine constants. It is found that the isotropic part of the Mu^* hyperfine interaction is negative, indicating the importance of exchange polarization. The transition rate from Mu to Mu^* follows an Arrhenius law over more than four decades. Finally, data are presented on the temperature dependence of the hyperfine interaction of isotropic Mu in diamond.

I. INTRODUCTION

Positive muons implanted into insulators and semiconductors often bind an electron to form Mu, a paramagnetic atom electronically similar to hydrogen but with approximately one-ninth the mass.¹ This state is characterized by an isotropic hyperfine interaction which may be significantly weaker than that of muonium in vacuum. In the semiconductors diamond,² silicon,^{3,4} germanium,⁵ GaP and GaAs,⁶ an additional muonium state, Mu^* , is observed whose hyperfine interaction has [111]-axial symmetry. The hyperfine interaction of Mu^* is in general strongly anisotropic, and its isotropic part A_s is more than 1 order of magnitude weaker than that of vacuum Mu.

The electron spin density at the muon is reflected by A_s , hence, knowledge of its sign is required in order to construct a realistic model of Mu^* . For example, a positive spin density might indicate that a single paramagnetic electron occupies an orbital which is centered on the muon, while a negative spin density suggests that initially diamagnetic electrons at the muon are exchange polarized by a more distant paramagnetic electron. In this paper, an investigation is presented of the thermally activated transition² from the isotropic Mu state to the anisotropic Mu^* state in diamond which allows an experimental determination of the sign of A_s .

The spin Hamiltonian for the isotropic Mu state in an external field \mathbf{B} is given by

$$H = h A \mathbf{I} \cdot \mathbf{S} - g_\mu \mu_\mu \mathbf{I} \cdot \mathbf{B} - g_e \mu_B \mathbf{S} \cdot \mathbf{B}, \quad (1)$$

where \mathbf{I} and \mathbf{S} are the muon and electron spin operators, respectively, and A is the hyperfine frequency. For Mu in vacuum $A_{\text{vac}} = 4463$ MHz, and for Mu in diamond at low temperature² $A = 3711$ MHz. In this paper, we present measurements of $A(T)$ in diamond up to 398 K.

The spin Hamiltonian⁷ for the anisotropic Mu^* state

differs from Eq. (1) by the addition of an anisotropic term:

$$\begin{aligned} \tilde{H} = & h A_\parallel \mathbf{I} \cdot \mathbf{S} + h (A_\parallel - A_\perp) (\mathbf{I} \cdot \hat{\mathbf{n}}) (\mathbf{S} \cdot \hat{\mathbf{n}}) \\ & - g_\mu \mu_\mu \mathbf{I} \cdot \mathbf{B} - g_e \mu_B \mathbf{S} \cdot \mathbf{B}. \end{aligned} \quad (2)$$

Here $\hat{\mathbf{n}}$ is a unit vector along one of the four equivalent [111] axes in the diamond lattice. It is convenient to express the Mu^* hyperfine constants A_\parallel and A_\perp in terms of the isotropic and anisotropic contributions $A_s = (A_\parallel + 2A_\perp)/3$ and $A_p = (A_\parallel - A_\perp)/3$. For Mu^* in diamond, μ SR measurements extrapolated to 0 K yield $|A_s| = 205.7$ MHz and $|A_p| = 186.6$ MHz, with A_s and A_p of opposite sign.

At low temperatures, both the Mu and Mu^* states are observed in diamond. With increasing temperature, first the Mu signals disappear, and at still higher temperatures the Mu^* signals become stronger. Zero-field measurements of the temperature-dependent Mu^* signal strength in a powder sample² demonstrated that a thermally-activated transition occurs from the Mu to the Mu^* state, adding to the "prompt" Mu^* fraction seen at lower temperature. Soon after this observation it was suggested⁸ that measurements on a single crystal would show a resonant transfer of the muon polarization at applied magnetic fields where Mu and Mu^* precession frequencies coincide and that such a resonance could be used to determine the sign of the Mu^* hyperfine parameters (relative to that of the isotropic state, taken to be positive). Such a measurement was attempted, but since the sample was rich in nitrogen (type Ia), rapid Mu relaxation due to impurity trapping prevented an unambiguous sign determination.⁹

We have performed this resonance experiment on a nitrogen-poor crystal of type IIb. This leads to narrow precession lines and a sharp resonance, as required for a conclusive sign determination. Furthermore, the elimina-

tion of Mu trapping allowed us to follow the transition from the decay of the precursor Mu state to the enhancement of the product Mu* signals and to describe both processes with a *single* Arrhenius law. A preliminary report of these experiments has been presented elsewhere.¹⁰ The large temperature region over which Mu signals could be observed in this sample also permitted us to observe the variation of the Mu hyperfine frequency with temperature.

II. THEORY

Assuming that the muon captures spin-up and spin-down electrons with equal probability, the spin-density matrix for a muonium state at time zero is given by

$$\rho(0) = \frac{1}{4} [1 + \mathbf{p}_\mu(0) \cdot \boldsymbol{\sigma}], \quad (3)$$

where $\boldsymbol{\sigma} = \frac{1}{2} \mathbf{I}$ are the Pauli spin matrices and $\mathbf{p}_\mu(0)$ is the initial muon polarization. With the expression

$$\rho(t) = \exp(-iHt/\hbar) \rho(0) \exp(iHt/\hbar) \quad (4)$$

for the time dependence of the density matrix, the muon polarization at later times is obtained from

$$\mathbf{p}(t) = \text{Tr}[\rho(t)\boldsymbol{\sigma}]. \quad (5)$$

The muon polarization oscillates at frequencies ω_{mn} given by differences in the hyperfine energy levels:

$$\omega_{mn} = 2\pi\nu_{mn} = (E_m - E_n)/\hbar. \quad (6)$$

Here we denote by E_m the energy eigenvalue of the eigenstate $|m\rangle$ of H ($H|m\rangle = E_m|m\rangle$). We now assume that this "precursor" muonium state undergoes a transition at a rate Λ to a different "final" state described by a spin Hamiltonian \tilde{H} . The spin dynamics of such transitions have been treated by Percival and Fischer¹¹ and by Meier.⁸ The resulting muon polarization is given by

$$\mathbf{p}_{\text{tot}}(t) = \mathbf{p}(t) \exp(-\Lambda t) + \mathbf{p}_{\text{tr}}(t) \quad (7)$$

with

$$\mathbf{p}_{\text{tr}}(t) = \Lambda \int_0^t dt' \exp(-\Lambda t') \text{Tr} \{ \exp[-i\tilde{H}(t-t')/\hbar] \rho(t') \times \exp[i\tilde{H}(t-t')/\hbar] \cdot \boldsymbol{\sigma} \}. \quad (8)$$

If the muon polarization is carried over from one state to the other but the electron polarization is lost, the density matrix at the time of the reaction t' is given by

$$\rho(t') = \frac{1}{4} [1 + \mathbf{p}(t') \cdot \boldsymbol{\sigma}]. \quad (9)$$

If, on the other hand, the electron polarization is also conserved during the transition, as is generally the case in radical termination reactions,¹² then $\rho(t')$ is given by Eq. (4) with $t = t'$. Integrating over all transition times t' , one obtains¹¹

$$\begin{aligned} \mathbf{p}_{\text{tot}}(t) = & \sum_{m,n,\tilde{m},\tilde{n}} [\langle m | \rho(0) | n \rangle \langle n | \boldsymbol{\sigma} | m \rangle - \mathbf{P}_{\tilde{m},\tilde{n}/m,n} \exp(i\alpha_{mn}^{\tilde{m}\tilde{n}})] \exp[-(i\omega_{mn} + \Lambda)t] \\ & + \sum_{m,n,\tilde{m},\tilde{n}} \mathbf{P}_{\tilde{m},\tilde{n}/m,n} \exp(-i\tilde{\omega}_{\tilde{m}\tilde{n}}t + i\alpha_{mn}^{\tilde{m}\tilde{n}}), \end{aligned} \quad (10)$$

where

$$\mathbf{P}_{\tilde{m},\tilde{n}/m,n} = \langle \tilde{m} | m \rangle \langle m | \rho(0) | n \rangle \langle n | \tilde{n} \rangle \langle \tilde{n} | \boldsymbol{\sigma} | \tilde{m} \rangle \cos \alpha_{mn}^{\tilde{m}\tilde{n}} \quad (11)$$

and

$$\tan \alpha_{mn}^{\tilde{m}\tilde{n}} = \frac{\tilde{\omega}_{\tilde{m}\tilde{n}} - \omega_{mn}}{\Lambda}. \quad (12)$$

Two points should be noted: (i) The damping rate of the precursor precession signals (at the frequencies ω_{mn}) is simply the transition rate Λ . (ii) The amplitudes of the final-state signals ($\tilde{\omega}_{\tilde{m}\tilde{n}}$) are sensitive to the angle α and show a maximum when $\alpha = 0$ (i.e., when $\tilde{\omega}_{\tilde{m}\tilde{n}} = \omega_{mn}$).

We apply this description to the case of a Mu \rightarrow Mu* transition, where the angle θ between the Mu* symmetry axis \mathbf{n} and the applied field \mathbf{B} is 90° and where the electron polarization is conserved. The indices of the hyperfine energy eigenstates for both Mu and Mu* are taken to be those used in Ref. 2. There are two particular values $B_- \simeq 15.4$ mT and $B_+ \simeq 17.2$ mT of the field where the precursor Mu precession frequencies coincide with the 1-2 Mu* line (see Fig. 1). If the Mu hyperfine in-

teraction is taken to be positive (by analogy with vacuum Mu), then a resonantly large fraction of the muon polarization will be carried over from Mu to Mu* at either B_- or B_+ , depending upon whether $A_s(\text{Mu}^*)/A(\text{Mu})$ is less than or greater than zero. The Mu* 3-4 signal precesses in the opposite sense and thus does not produce a resonance.

The existence of a single resonant field follows from the assumption that the electron polarization is conserved during the transition. Due to the smallness of the Mu* hyperfine coupling constants, the Mu* electron spin is decoupled from the muon at magnetic fields greater than ~ 10 mT. For $A_s(\text{Mu}^*)/A(\text{Mu}) > 0$, the Mu* precession signal $\tilde{\omega}_{12}$ then corresponds to a muon spin flip with the electron spin up, and for $A_s(\text{Mu}^*)/A(\text{Mu}) < 0$ to the electron spin down. Further, the Mu hyperfine states $|1\rangle$ and $|3\rangle$ are also eigenstates of S_z with the electron spin up and down, respectively. The factors $\langle \tilde{m} | m \rangle$ and $\langle n | \tilde{n} \rangle$ in Eq. (11) thus imply that a coincidence between $\tilde{\omega}_{12}$ and ω_{12} ($\tilde{\omega}_{12}$ and ω_{23}) will cause a resonant polarization transfer for $A_s(\text{Mu}^*)/A(\text{Mu}) > 0$ (< 0). In the *absence* of electron spin conservation this selection does not occur, and an enhanced transfer of muon polarization is expected at *both* B_- and B_+ .

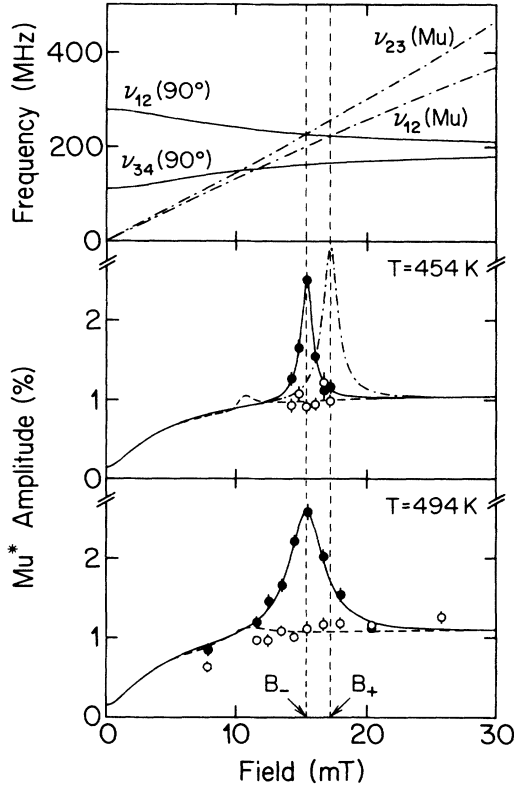


FIG. 1. Expected Mu and Mu* precession frequencies for the magnetic field along the [110] axis in diamond. Also shown are the measured and fitted amplitudes of the Mu* precession signals 1-2 (solid circles, solid curves) and 3-4 (open circles, dashed curves) as a function of the applied field at 454 and 494 K. The resonant maximum at the field $B_- = 15.4$ mT establishes that $A_s(\text{Mu}^*)/A(\text{Mu}) < 0$. For comparison, the dot-dashed curve shows the expected resonance at B_+ for the opposite sign (> 0).

III. EXPERIMENTAL DETAILS

The muon spin rotation technique has been described earlier.¹ The experiments were performed at the Swiss Institute for Nuclear Research (SIN) using 28 MeV/c muons on a single-crystal diamond sample with no evidence of nitrogen impurities in its infrared absorption spectrum. The diamond was in a high-vacuum hot finger oven with the applied magnetic field along [110]. Fine orientation adjustments of the crystal were made based on the Mu* line splitting. In this orientation, two [111] symmetry axes are at $\theta = 90^\circ$, and the other two are at $\theta = 35.26^\circ$ with respect to the external field. The measurements were performed in the temperature region 300–600 K, and magnetic fields up to 25 mT were applied. The uncertainty of the sample temperature was less than 0.1 K and that of the field less than 0.4%. To minimize background, muon decay positrons were detected perpendicular to the incoming beam. Our time resolution of approximately 900 ps FWHM allowed the observation of frequencies up to 500 MHz. In each run, $2\text{--}5 \times 10^6$ good muon decay events were accumulated in each of two time histograms, of which approximately

20% were from muons which stopped in the copper target holder. The precession frequencies, their amplitudes and their relaxation rates were extracted by multifrequency fits to the μSR time histograms. The transition model [Eqs. (10)–(12)] was fitted to the weighted average of the amplitudes from both histograms and corrected for the finite time resolution. In the analysis, account was taken of the temperature dependence of the Mu* hyperfine constants.²

IV. RESULTS

A. Sign determination of A_s

Assuming electron-spin conservation, a field scan at constant temperature should yield a 1-2 Mu* precession amplitude with a resonant maximum at either B_- or B_+ , depending on the sign of A_s . The width of this resonance is a function of the transition rate and therefore temperature dependent; a sign determination requires a narrow resonance and, hence, a measurement at as low a temperature as possible. Field scans were performed at 454 and 494 K, and the field was varied in the vicinity of the frequency crossing. Combined fits of the transition model to the amplitudes of both $\theta = 90^\circ$ Mu* lines were made under the assumptions that a temperature-independent “prompt” Mu* fraction f_1 is always present and that a Mu fraction f_2 is a precursor for Mu*. Note that with the [110] crystal orientation, there are two 90° Mu* centers whose contributions must be added in phase.

The amplitude of the 1-2 Mu* line showed a single resonance at B_- (see Fig. 1), establishing that the electron polarization is conserved during the transition and that the isotropic part A_s of the Mu* hyperfine interaction is *negative* (and hence that A_p is positive). For comparison, the dot-dashed curve in the figure shows the expected results for a positive A_s and negative A_p and unchanged values for the other fit parameters. The fitted transformation rate Λ was found to be $46(5) \times 10^6 \text{ s}^{-1}$ at 454 K and $142(12) \times 10^6 \text{ s}^{-1}$ at 494 K.

B. Temperature dependence of the Mu \rightarrow Mu* transition rate

As mentioned above, in the absence of additional depolarization such as from trapping at impurities, the damping rate of the precursor Mu state is equal to the Mu \rightarrow Mu* transition rate Λ . The temperature dependence of the Mu relaxation rate was studied in the range 300 to 400 K in an applied field of 1.25 mT. At this low field, the Mu precession frequencies ν_{12} and ν_{23} are centered at 17.1 MHz with an unresolved splitting of ~ 0.18 MHz. With account taken of the splitting, a fit of the Mu relaxation rate λ to the Arrhenius law

$$\lambda(T) = \Lambda(T) + \lambda_0 = \Psi \exp(-U/kT) + \lambda_0 \quad (13)$$

yielded the dot-dashed curve in Fig. 2. λ_0 denotes a temperature-independent background.

At still higher temperatures, the transition rate Λ can be determined from the temperature-dependent increase of the Mu* amplitude. Such measurements were per-

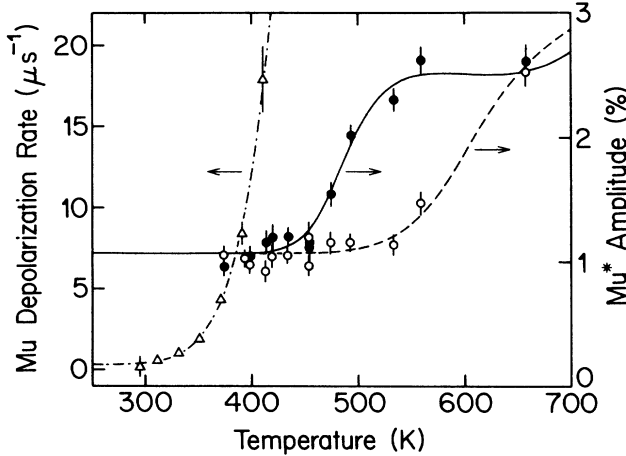


FIG. 2. Mu damping rate for a field of 1.25 mT (triangles and left-hand scale) as a function of sample temperature. The dot-dashed curve is a fit to an Arrhenius law. Also shown are the measured amplitudes of the 1-2 (solid circles) and 3-4 open circles) precession signals for $\theta=90^\circ$ Mu^* centers in a field of 16.5 mT (right-hand scale). The solid and dashed curves are fits to the $\text{Mu} \rightarrow \text{Mu}^*$ transition model assuming the same Arrhenius law for the transition rate.

formed from 300 to 600 K in an applied field of 16.5 mT, i.e., between the crossover fields B_- and B_+ . The measured $\theta=90^\circ$ Mu^* precession amplitudes are presented in Fig. 2. The constant value for $T < 400$ K corresponds to the prompt Mu^* fraction f_1 . The shift of the rise in the 3-4 amplitude to higher temperatures is a consequence of its opposite sense of precession. A second increase of the Mu^* amplitudes, from the transfer of Mu polarization components at higher frequencies (> 3 GHz) is expected above 670 K. The solid and dashed curves in Fig. 2 are the results of a fit to the transition model assuming an Arrhenius law for Λ .

Values of $\Lambda(T)$ are thus available from the field-dependent Mu^* amplitude, the temperature-dependent Mu relaxation rate, and the temperature-dependent Mu^* amplitudes. A global fit to these values (see Fig. 3) was performed to an Arrhenius law with the resulting values

$$\begin{aligned} \Psi &= 1.14(28) \times 10^{13} \text{ s}^{-1}, \\ U &= 0.476(9) \text{ eV}. \end{aligned} \quad (14)$$

The entire muon polarization in the nitrogen-poor diamond at room temperature could be accounted for by the prompt Mu^* fraction $f_1=25(2)\%$ and the precursor Mu fraction $f_2=75(6)\%$. Any missing fraction was less than 6%. The temperature-independent quotient f_1/f_2 obtained as a weighted average from all the measurements was 0.328(12).

C. Temperature dependence of the Mu hyperfine parameter

The temperature dependences of the Mu hyperfine parameter in Si and Ge have been measured with the sensitive zero-field, high-time-resolution technique.¹³ No measurement of $A(T)$ for Mu in diamond has yet been re-

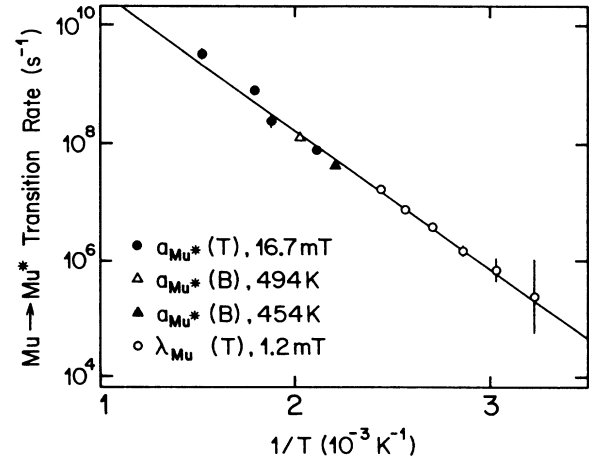


FIG. 3. Experimental values of the temperature-dependent $\text{Mu} \rightarrow \text{Mu}^*$ transition rate Λ obtained from the indicated experiments. The solid line is a fit to an Arrhenius law.

ported. In our nitrogen-poor sample, we observed Mu precession at the frequencies ν_{12} and ν_{23} above room temperature in fields up to 45.3 mT. Together with the precession frequency $\nu_\mu = 135.54 \text{ MHz}/T \times B$ of free muons, these measurements yield the Mu hyperfine frequency A according to

$$A = 2 \left[\frac{\nu_{12}\nu_{23} + \nu_\mu(\nu_{12} + \nu_{23} + \nu_\nu)}{\nu_{23} - \nu_{12}} \right]. \quad (15)$$

Under the assumption that the muon g factor g_μ is not appreciably influenced by the solid host, we obtain in addition the electronic g factor g_e from the relation

$$g_e = -g_\mu \frac{m_e}{m_\mu} \left[\frac{\nu_{12} + \nu_{23}}{\nu_\mu} + 1 \right]. \quad (16)$$

The experimental values for A and g_e are summarized in Table I. Because of the limited data available, we cannot discriminate between the Debye and the Einstein models for $A(T)$ discussed in Refs. 2 and 14.

V. CONCLUSIONS

Our study of the $\text{Mu} \rightarrow \text{Mu}^*$ transition in diamond clearly establishes that the isotropic part of the Mu^* hyperfine interaction is negative. This implies that Mu^*

TABLE I. The hyperfine coupling constant A and electronic g factor g_e for isotropic Mu in a nitrogen-poor diamond as function of temperature.

T (K)	A (MHz)	g_e
6 ^a	3711(21)	-2.0034(17)
293.0	3710.9(1.0)	-1.9971(56)
373.5	3693.0(8.6)	-1.9972(57)
398.5	3568(69)	-2.005(12)

^aTaken from Ref. 2.

is not simply a distorted version of isotropic Mu, since this would require a positive electron spin density at the muon. A more promising model of Mu* is a paramagnetic complex similar to a molecular radical with the unpaired electron removed from the muon. The weak negative spin density at the muon is then the result of an "exchange polarization" mechanism. The Mu* hyperfine constants A_s and A_p have been studied previously in diamond, silicon and germanium as a function of temperature.¹⁵ Although in that work the incorrect sign for A_s was assumed, in view of the similar behavior for the three materials, it was convincingly argued that the same sign assignments for A_s and A_p should apply. A further result of the present investigation is that the thermally-activated transition from Mu to Mu* in diamond proceeds without loss of the electron polarization.

At room temperature, Mu and Mu* are observed simultaneously in the μ SR spectra; both are formed promptly upon muon implantation. The thermally-activated conversion of Mu to Mu*, together with the fact that Mu* is observable² in diamond up to at least 1100 K establishes that Mu* is the more stable state (in Si and Ge, Mu* disappears above 165 and 85 K, respectively, perhaps under the influence of free carriers^{16,17}).

While normal muonium is generally accepted to be at a tetrahedral interstitial site in the diamond lattice,¹⁸⁻²⁵ the site of Mu* is still uncertain. The anisotropic hyperfine interaction of Mu* implies that it is immobile. Of the many models that have been suggested for Mu*, the two models which are being most seriously developed are (i) muonium which occupies a host-ion vacancy²⁶⁻³⁰

and (ii) muonium situated near the center of a host bond.³¹⁻³⁵ Both of these models appear consistent with $A_s < 0$, but the high Arrhenius prefactor $\Psi \approx 10^{13} \text{ s}^{-1}$ for the Mu \rightarrow Mu* transition rate $\Lambda(T)$ is incompatible with a model where the precursor Mu searches for a preexisting lattice vacancy in order to become Mu*. This value for Ψ is comparable to an optical phonon frequency in diamond and, hence, is approximately the maximum possible jump rate for Mu, implying that only a *single jump* is required by Mu to form Mu*. A cluster calculation^{33,35} of the potential energy surface traversed by muonium from the tetrahedral interstitial site to the center of a strongly stretched C—C bond in diamond reproduces our observation that the Mu state is metastable but apparently overestimates the true barrier height. Further support of the bond-centered model for Mu* has been provided by the observation of its resolved nuclear hyperfine structure in Si,³⁶ and with a single Ga and a single As in GaAs.³⁷

ACKNOWLEDGMENTS

We would like to thank Professor P. F. Meier for stimulating discussions in the preliminary stages of this work. This work was supported by SIN and the Swiss National Science Foundation. Three of the authors (J.P.F.S., M.C.S., and S.C.) acknowledge support from the University of the Witwatersrand and one author (D.P.S.) acknowledges support from the U.S. National Science Foundation.

*Permanent address: Pritzker School of Medicine, University of Chicago, Chicago, IL 60637.

¹B. D. Patterson, in *Muons and Pions in Materials Research*, edited by J. Chappert and R. I. Grynspan (North-Holland, Amsterdam, 1984), p. 161.

²E. Holzschuh, W. Kündig, P. F. Meier, B. D. Patterson, J. P. F. Sellschop, M. C. Stemmet, and H. Appel, *Phys. Rev. A* **25**, 1272 (1982).

³J. H. Brewer, K. M. Crowe, F. N. Gyax, R. F. Johnson, B. D. Patterson, D. G. Fleming, and A. Schenck, *Phys. Rev. Lett.* **31**, 143 (1973).

⁴B. D. Patterson, A. Hintermann, W. Kündig, P. F. Meier, F. Waldner, H. Graf, E. Recknagel, A. Weidinger, and Th. Wichert, *Phys. Rev. Lett.* **40**, 1347 (1978).

⁵E. Holzschuh, H. Graf, E. Recknagel, A. Weidinger, Th. Wichert, and P. F. Meier, *Phys. Rev. B* **20**, 4391 (1979).

⁶R. F. Kiefl, J. W. Schneider, H. Keller, W. Kündig, W. Odermatt, P. D. Patterson, K. W. Blazey, T. L. Estle, and S. L. Rudaz, *Phys. Rev. B* **32**, 530 (1985).

⁷We follow the notation of Ref. 8, using the relations $A_{\perp} = \omega_0/2\pi$ and $A_{\parallel} = (\omega_0 + \omega^*)/2\pi$ for the hyperfine constants.

⁸P. F. Meier, *Phys. Rev. A* **25**, 1287 (1982).

⁹B. D. Patterson, E. Holzschuh, W. Kündig, P. F. Meier, W. Odermatt, J. P. F. Sellschop, and M. C. Stemmet, *Hyperfine Interact.* **17-19**, 605 (1984).

¹⁰W. Odermatt, Hp. Baumeler, H. Keller, W. Kündig, B. D. Patterson, J. W. Schneider, J. P. F. Sellschop, M. C. Stemmet,

and S. Connell, *Hyperfine Interact.* **32**, 583 (1986).

¹¹P. W. Percival and H. Fischer, *Chem. Phys.* **16**, 89 (1976).

¹²H. Fischer and H. Paul, *Acc. Chem. Res.* **20**, 200 (1987).

¹³E. Holzschuh, *Phys. Rev. B* **27**, 102 (1983).

¹⁴K. W. Blazey, J. A. Brown, D. W. Cooke, S. A. Dodds, T. L. Estle, R. H. Heffner, M. Leon, and D. A. Vanderwater, *Phys. Rev. B* **23**, 5316 (1981).

¹⁵K. W. Blazey, T. L. Estle, E. Holzschuh, W. Odermatt, and B. D. Patterson, *Phys. Rev. B* **27**, 15 (1983).

¹⁶A. Weidinger, G. Balzer, H. Graf, E. Recknagel, and Th. Wichert, *Phys. Rev. B* **24**, 6185 (1981).

¹⁷E. Albert, A. Möslang, E. Recknagel, and A. Weidinger, *Hyperfine Interact.* **17-19**, 611 (1984).

¹⁸M. Manninen and P. F. Meier, *Phys. Rev. B* **26**, 6690 (1982).

¹⁹N. Sahoo, S. K. Mishra, A. Coker, T. P. Das, C. K. Mitra, L. C. Snyder, and A. Glodeanu, *Phys. Rev. Lett.* **50**, 913 (1983).

²⁰H. Katayama-Yoshida and K. Shindo, *Phys. Rev. Lett.* **51**, 207 (1983).

²¹S. Estreicher, A. K. Ray, J. L. Fry, and D. S. Marynick, *Phys. Rev. Lett.* **55**, 1976 (1985).

²²S. Estreicher and D. S. Marynick, *Hyperfine Interact.* **32**, 613 (1986).

²³S. Estreicher, A. K. Ray, J. L. Fry, and D. S. Marynick, *Phys. Rev. B* **34**, 6071 (1986).

²⁴N. Sahoo, K. C. Mishra, and T. P. Das, *Phys. Rev. Lett.* **57**, 3300 (1986).

²⁵S. Estreicher, A. K. Ray, J. L. Fry, and D. S. Marynick, *Phys. Rev. Lett.* **57**, 3301 (1986).

- ²⁶T. L. Estle, *Hyperfine Interact.* **17-19**, 585 (1984).
- ²⁷N. Sahoo, K. C. Mishra, and T. P. Das, *Phys. Rev. Lett.* **55**, 1506 (1985).
- ²⁸S. Estreicher and D. S. Marynick, *Phys. Rev. Lett.* **56**, 1511 (1986).
- ²⁹N. Sahoo, K. C. Mishra, and T. P. Das, *Phys. Rev. Lett.* **56**, 1512 (1986).
- ³⁰N. Sahoo, K. C. Mishra, and T. P. Das, *Hyperfine Interact.* **32**, 619 (1986).
- ³¹M. C. R. Symons, *Hyperfine Interact.* **17-19**, 771 (1984).
- ³²S. F. J. Cox and M. C. R. Symons, *Chem. Phys. Lett.* **126**, 516 (1986).
- ³³T. A. Claxton, A. Evans, and M. C. R. Symons, *J. Chem. Soc. Faraday Trans. 2* **82**, 2031 (1986).
- ³⁴T. L. Estle, S. Estreicher, and D. S. Marynick, *Hyperfine Interact.* **32**, 637 (1986).
- ³⁵T. L. Estle, S. Estreicher, and D. S. Marynick, *Phys. Rev. Lett.* **58**, 1547 (1987).
- ³⁶R. F. Kiefl, M. Celio, T. L. Estle, S. R. Kreitzman, G. M. Luke, T. M. Riseman, and E. J. Ansaldo, *Phys. Rev. Lett.* **60**, 224 (1988).
- ³⁷R. F. Kiefl, M. Celio, T. L. Estle, G. M. Luke, S. R. Kreitzman, J. H. Brewer, D. R. Noakes, E. J. Ansaldo, and K. Nishiyama, *Phys. Rev. Lett.* **58**, 1780 (1987).